Zuschriften

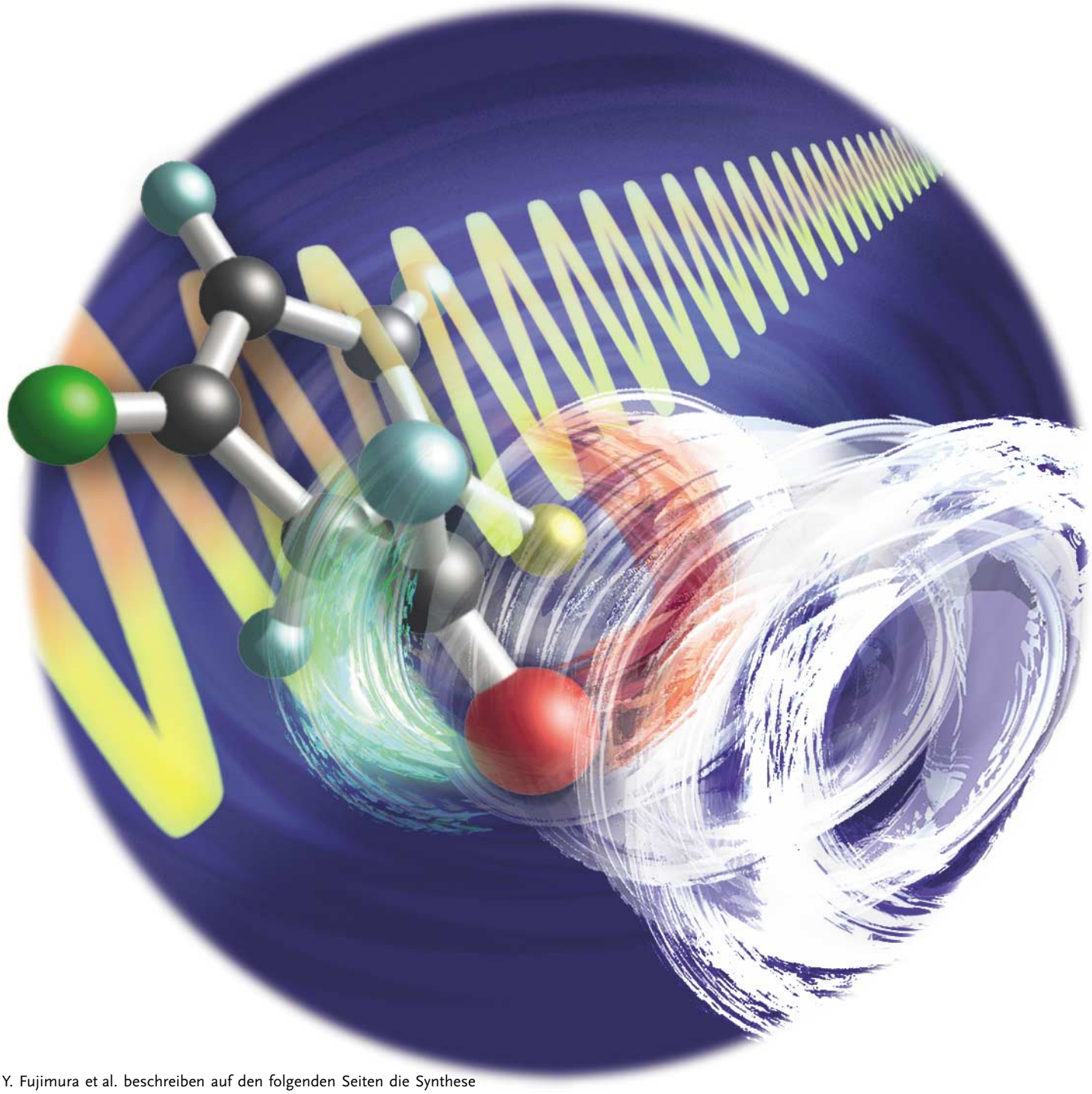

Y. Fujimura et al. beschreiben auf den folgenden Seiten die Synthese eines chiralen molekularen Motors. Die Rotation dieses Motors wird durch das kohärente elektromagnetische Feld eines nichthelicalen Laserpulses angetrieben und erfolgt in nur einer Drehrichtung. Rechnungen auf der Basis von klassischer Mechanik und Quantenmechanik erklären das Phänomen.

DOI: 10.1002/ange.200250872

Molecular Motors

Chiral Molecular Motors Driven by a Nonhelical Laser Pulse**

*Kunihito Hoki, Masahiro Yamaki, and Yuichi Fujimura**

The field of molecular motors and machines is one of the most rapidly advancing research areas in applied chemistry.[1–4] It is expected that this area will play an important role in the advent of nanoscience and nanotechnology. Most of the molecular motors reported to date have been made from chiral molecules that have asymmetric potentials. Furthermore, these motors are driven by concentration gradients that are created by thermal and chemical forces, or by the time-correlated forces of electromagnetic radiation.[5–9] Light-driven molecular motors are particularly interesting because their rotational directions, as well as their torque, can be controlled by utilizing the properties of light, such as photon polarization, frequency, and pulse shape.[10,11] For example, a grid-mounted molecular dipolar rotor, driven by a circularly polarized electric field, has been theoretically studied on the basis of classical molecular dynamics.[6] It should be noted that if helical light fields, such as circularly polarized lasers are used, the chirality of the molecular motors is unnecessary.[12] Interesting experiments regarding nonhelical-light-driven chiral molecular motors have recently been reported;[8,9] such motors consist of an alkene with two chiral centers. *cis–trans* Isomerization that is induced by linearly polarized visible or UV light generates repetitive unidirectional rotation around a central carbon–carbon double bond, which is followed by thermally induced *cis–trans* isomerization; the latter blocks reverse rotation. In those experiments, the rate-determining step of the motor action is the thermally controlled isomerization, which is an incoherent process.[8,9] To the best of our knowledge, there are only a few reports on molecular motors driven by using the coherent properties of radiation fields. Investigation of molecular motors driven by the coherent properties of electromagnetic fields is therefore required.

In this communication, on the basis of both quantum and classical mechanical calculations, we explain how a chiral molecular motor is unidirectionally driven by a nonhelical coherent light pulse. For this purpose, 2-chloro-5-methylcyclopenta-2,4-dienecarbaldehyde was chosen (Figure 1), which is a simple, chiral molecular motor. In this communication, chiral molecules with an *R* formation are called (*R*)-motors, and those with an *S* formation are termed (*S*)-motors. The dihedral angle α between the O^1–C^2–C^3 and C^2–C^3–H^4 planes is set to be variable of the internal rotation of the CHO group around the C^2–C^3 bond.

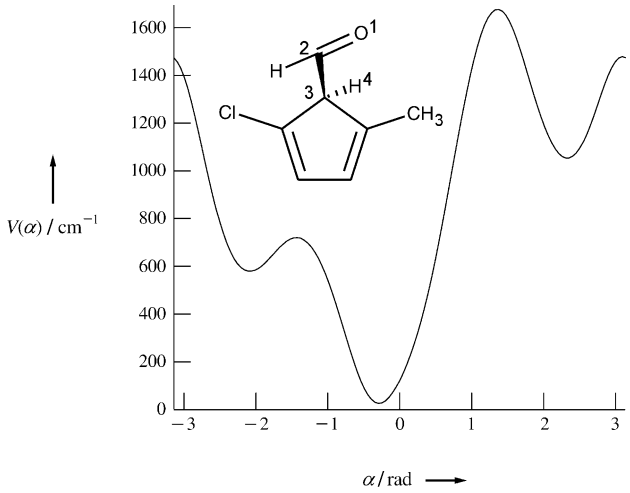

Figure 1. The potential energy of an (*R*)-motor as a function of the internal rotation coordinate α. The (*R*)-motor is also shown. The CHO group around the C^2–C^3 bond is considered as the engine of the motor, which is driven by a linearly polarized laser pulse.

Figure 1 shows the potential energy of the (*R*)-motor as a function of α. This chiral molecule has several properties that are essential for a molecular motor. First, the potential energy $V(\alpha)$ is asymmetric, as shown in Figure 1. The potential is most stable at $\alpha = -0.26$ rad. The potential slope is gentle between $\alpha = -0.26$ and -1.3 rad, and in contrast is steep between $\alpha = -0.26$ and 1.3 rad.

Secondly, the components of the dipole moment vector $\boldsymbol{\mu}(\alpha)$ vary greatly with different values of α because of the electronegativity of the O^1 atom. The difference between the maximum and minimum of the components of the dipole moment vector is nearly 4 D.[12] Dipole interactions with electric fields of a few GV m^{-1} compare to a potential barrier height of 1600 cm^{-1}. The values of $V(\alpha)$ and $\boldsymbol{\mu}(\alpha)$ were calculated using an ab initio MO method.[13]

Thirdly, the rotational constants are 1.97, 1.16, and 0.79 GHz. Thus, the effects of molecular rotation with periods of a few hundred picoseconds can be safely ignored, since the molecular-motor dynamics of interest occur within several tens of picoseconds.

The Hamiltonian of the molecular motor in a laser field $\boldsymbol{E}(t)$ is expressed as:

$$\mathscr{H}(t) = -\frac{\hbar^2}{2I}\frac{\partial^2}{\partial\alpha^2} + V(\alpha,t) \qquad (1)$$

Here, I is the moment of inertia of internal rotation. The total potential including the molecule–radiation field interaction $V(\alpha,t)$ is expressed within the dipole approximation as:

$$V(\alpha,t) = V(\alpha) - \mu(\alpha)\cdot\boldsymbol{E}(t) \qquad (2)$$

[*] Prof. Y. Fujimura, K. Hoki, M. Yamaki
Department of Chemistry
Graduate School of Science, Tohoku University
Sendai 980-8578 (Japan)
Fax: (+81) 22-217-7715
E-mail: fujimura@mcl.chem.tohoku.ac.jp

[**] This work was partly supported by Grant-in-Aid for Scientific Research on Priority Areas, "Control of Molecules in Intense Laser Fields" (Area No. 419) from the Ministry of Education, Science and Culture, Japan. One of the authors (K.H.) acknowledges support from a Research Fellowship of the JSPS (No. 6254).

  DOI: 10.1002/ange.200250872

The time evolution of the molecular state, $\Psi(t)$, is estimated by solving the time-dependent Schrödinger equation:

$$i\hbar\frac{\partial}{\partial t}\Psi(t) = \mathscr{H}(t)\,\Psi(t) \tag{3}$$

As a measure of molecular-motor action, we introduce a quantum mechanical expectation value of the angular momentum operator of the internal rotation, $\langle \ell(t)\rangle$, defined as:

$$\langle \ell(t)\rangle = \int_0^{2\pi} \mathrm{d}\alpha\, \Psi(t)^*\left(-i\hbar\frac{\partial}{\partial\alpha}\right)\Psi(t) \tag{4}$$

Here, the sign and absolute quantity of the expectation value correspond to the direction of the angular momentum and its magnitude, respectively.

Figure 2b shows values for $\langle \ell(t)\rangle$ calculated for an (*R*)-motor driven by a linearly polarized laser pulse in the *Z* direction at the low-temperature limit.[14] The envelope of the electric field of the pulse used is shown in Figure 2a. For simplicity, the body of the molecular motor was fixed at a space: the direction of the C^2–C^3 bond is parallel to the *z* axis, and the angle between the C^3–H^4 bond, projected onto the *yz* plane and the *z* axis is 0.1π, at which angle the laser pulse strongly interacts with the motor. Figure 2b shows that the direction of rotation is unidirectional, as suggested by the gentle slope of the potential shown in Figure 1. Furthermore,

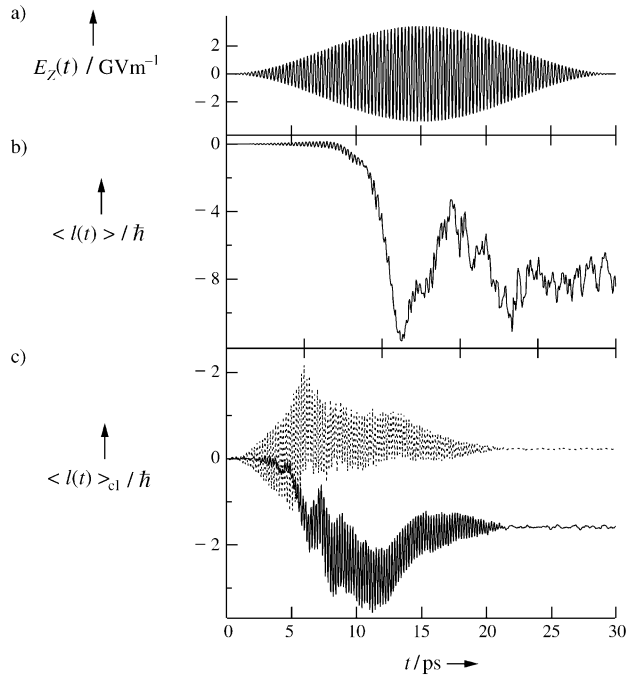

Figure 2. a) The electric field of a laser pulse that is linearly polarized to the *z* axis $E_z(t) = E_0 \sin^2(\pi t/t_f)\cos(\omega t)$ for $0 < t < t_f$ and $E_z(t) = 0$ for $t_f < t$. Here, $t_f = 30$ ps, $E_0 = 3.4$ GV m^{-1}, and $\omega = 124$ cm^{-1}; b) temporal behavior of the quantum-mechanically averaged angular momentum, $\langle \ell(t)\rangle$; c) temporal behavior of the averaged angular momentum based on classical mechanics, $\langle \ell(t)\rangle_{cl}$. The solid line shows the angular momentum of an (*R*)-motor, and the dotted line shows that of an analogous achiral molecule.

Figure 2b shows that the temporal behavior of the motor can be divided into three regimes: ignition, acceleration, and free rotation. In the ignition regime, the dynamics of the motor are characterized by the large amplitude vibration of a pendulum motion. In the second regime, the motor begins rotating unidirectionally and is accelerated by the applied laser pulse. The magnitude of $\langle \ell(t)\rangle$ follows the pulse envelope, as is qualitatively shown by comparing Figure 2a and b. Between the second and third regimes, such relationships start to break down. In the third regime, in which the driving laser pulse decreases in intensity and is eventually turned off, $\langle \ell(t)\rangle$ becomes a constant value (with some fluctuation) and the motor is in a steady state.

So far only the (*R*)-motor has been discussed. The (*S*)-motor can be considered similarly, as the potential energies of the (*S*)- and (*R*)-motors are mirror images of each other, with respect to a reflection plane located at $\alpha = 0$. The unidirectional motions of the (*S*)- and (*R*)-motors are opposite to each other. We obtained a value for $\langle \ell(t)\rangle$ of 9.4×10^{11} rad s^{-1} after the laser pulse ($t_f < t$).

To clarify the origin of the unidirectional motion shown in Figure 2b, the results can be presented based on Newton's laws of motion.[15] The initial ensemble was set to be a canonical ensemble at $T = 150$ K. In Figure 2c, the solid line shows the ensemble-averaged angular momentum, $\langle \ell(t)\rangle_{cl}$. The temporal behavior of $\langle \ell(t)\rangle_{cl}$ is similar to that shown in Figure 2b, except for its smaller magnitude, which arises mainly a result of temperature effects. To highlight the important role of the asymmetric shape of the potential, the dotted line in Figure 2c shows $\langle \ell(t)\rangle_{cl}$ for an achiral molecule, where a chlorine atom is substituted for the methyl group of the chiral molecule. In the case of the achiral molecule, unidirectional internal rotation is not created after the laser pulse is turned off. This indicates that the unidirectional internal rotation of the molecule driven by a linearly polarized laser pulse originates from molecular chirality. Figure 3 shows one of the classical trajectories of the molecular motor. Here, the values for $\alpha(0)$ (−0.27 rad) and the angular momentum $\ell(0)$ (7.1 $\hbar$) were set as initial conditions. Figure 3 shows that the motor dynamics consist again of three regimes (ignition, acceleration, and rotation), and that the motor begins moving unidirectionally toward negative values of the asymmetric potential, $\alpha(t)$, with a gentle slope near 13 ps, followed by a pendulum motion. The

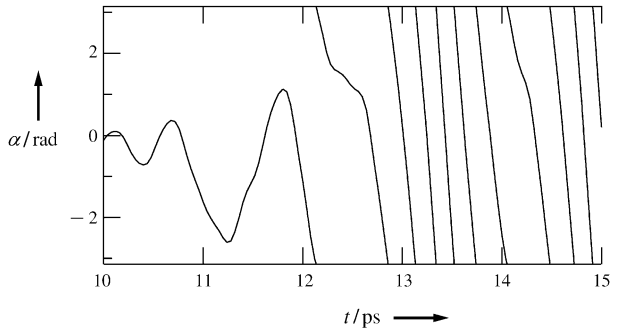

Figure 3. The classical trajectory of a chiral molecular motor, driven by a linearly polarized laser pulse.

shoulder appearing between 12 and 13 ps originates from climbing the "potential hump" located near $\alpha = 1.3$ rad.

In conclusion, the unidirectional rotation of chiral molecular motors driven by a nonhelical laser pulse has been explained on the basis of both quantum mechanical and classical mechanical calculations. The origin of the unidirectional rotation lies in both the asymmetric potential of chiral molecules and time-correlated forces created by laser–molecule interactions.[16] The results obtained in this study serve as a theoretical basis for the control of molecular motors with pulsed lasers. A further study of molecular motors taking into account damping effects will be presented elsewhere.

Received: December 30, 2002 [Z50872]

Keywords: chirality · laser chemistry · molecular dynamics · molecular motors · nanotechnology

[1] C. Joachim, J. K. Gimzewski in *Molecular Machines and Motors* (Ed.: J.-P. Sauvage), Springer, Berlin, **2001**, pp. 1–18; T. R. Kelly, J. P. Sestelo in *Molecular Machines and Motors* (Ed.: J.-P. Sauvage), Springer, Berlin, **2001**, pp. 19–53; L. Raehm, J.-P. Sauvage in *Molecular Machines and Motors* (Ed.: J.-P. Sauvage), Springer, Berlin, **2001**, pp. 55–78.
[2] J. K. Gimzewsky, C. Joachim, R. R. Schittler, V. Langlais, H. Tang, I. Johannesen, *Science* **1988**, *281*, 531–533.
[3] R. E. Tuzun, D. W. Niod, B. G. Sumpter, *Nanotechnology* **1995**, *6*, 52–63.
[4] V. Balzani, M. Gómez-López, J. F. Stoddart, *Acc. Chem. Res.* **1998**, *31*, 405–414.
[5] J.-P. Sauvage, *Acc. Chem. Res.* **1998**, *31*, 611–619.
[6] J. Vacek, J. Michl, *Proc. Natl. Acad. Sci. USA* **2001**, 98, 5481–5486.
[7] B. Space, H. Rabitz, A. Lörincz, P. Moore, *J. Chem. Phys.* **1996**, *105*, 9515–9524.
[8] N. Koumura, R. W. J. Zijlstra, R. A. van Delden, N. Harada, B. L. Feringa, *Nature* **1999**, *401*, 152–155.
[9] B. L. Feringa, N. Koumura, R. A. van Delden, M. K. J. Ter Wiel, *Appl. Phys. A* **2002**,75, 301–308.
[10] A. Assion, T. Baumert, M. Bergt, T. Brixner, B. Kiefer, V. Seyfried, M. Strehle, G. Gerber, *Science* **1998**, *282*, 919–922.
[11] T. Brixner, G. Gerber, *Opt. Lett.* **2001**, 26, 557–559.
[12] K. Hoki, M. Yamaki, S. Koseki, Y. Fujimura, *J. Chem. Phys.* **2003**, *118*, 497–504.
[13] Gaussian 98 (Revision A.7), M. J. Frisch, G. W. Trucks, H. B. Schlegel, G. E. Scuseria, M. A. Robb, J. R. Cheeseman, V. G. Zakrzewski, J. A. Montgomery, R. E. Stratmann, J. C. Burant, S. Dapprich, J. M. Millam, A. D. Daniels, K. N. Kudin, M. C. Strain, O. Farkas, J. Tomasi, V. Barone, M. Cossi, R. Cammi, B. Mennucci, C. Pomelli, C. Adamo, S. Clifford, J. Ochterski, G. A. Petersson, P. Y. Ayala, Q. Cui, K. Morokuma, D. K. Malick, A. D. Rabuck, K. Raghavachari, J. B. Foresman, J. Cioslowski, J. V. Ortiz, B. B. Stefanov, G. Liu, A. Liashenko, P. Piskorz, I. Komaromi, R. Gomperts, R. L. Martin, D. J. Fox, T. Keith, M. A. Al-Laham, C. Y. Peng, A. Nanayakkara, C. Gonzalez, M. Challacombe, P. M. W. Gill, B. G. Johnson, W. Chen, M. W. Wong, J. L. Andres, M. Head-Gordon, E. S. Replogle, J. A. Pople, Gaussian, Inc., Pittsburgh, PA, **1998**. The 6-31G(d) basis set and the MP2 method were used.
[14] See Ref. [12] for details of the calculations.
[15] The classically averaged angular momentum was obtained by using a Monte Carlo integration method with 10^6 trajectories.
[16] K. Hoki, M. Yamaki, S. Koseki, Y. Fujimura, unpublished results.

